Available online at www.sciencedirect.com

SCIENCE DIRECT®

Coastal Engineering 51 (2004) 439–454

Coastal Engineering
An International Journal for Coastal, Harbour and Offshore Engineers

www.elsevier.com/locate/coastaleng

Linear analysis of the multi-layer model

Patrick J. Lynett[a,*], Philip L.-F. Liu[b]

[a] Department of Civil Engineering, Texas A&M University, TAMU 3136, College Station, TX 77843-3136, USA
[b] School of Civil and Environmental Engineering, Cornell University, USA

Received 11 July 2003; received in revised form 27 April 2004; accepted 18 May 2004
Available online 3 August 2004

Abstract

A set of model equations for water wave propagation is derived by piecewise integration of the primitive equations of motion through N arbitrary layers. Within each layer, an independent velocity profile is determined. Depth-averaged and "extended" versions of the multi-layer model are presented and compared. With N separate velocity profiles, matched at the interfaces of the layers, the resulting set of "extended" equations have $2N-1$ free parameters, while the depth-averaged equations have $N-1$. A linear optimization is performed, showing that increasing the number of layers leads to better deep-water wave behavior.
© 2004 Elsevier B.V. All rights reserved.

Keywords: Boussinesq; High-order approximation; Velocity profiles

1. Introduction

Since the works of Madsen and Sorensen (1992) and Nwogu (1993), much of the developments in Boussinesq-type modeling have focused on extending the applicability of depth-integrated equations into deep water. Fundamentally, this extension is contrary to the physical basis on which one derives said equations. Boussinesq and Boussinesq-type models are typically based on a shallow-water scaling, and utilize an expansion in $\mu=kh$, requiring that μ is small. After the derivation is complete, this physical basis for derivation is in some part disregarded, and the model equations are applied to waves with $\mu>1$. For example, the equations of Madsen and Sorensen and Nwogu have good linear accuracy up to $\mu=3$, although nonlinear accuracy has very large errors outside of shallow water ($\mu>1$). This choice to apply the Boussinesq-type models into intermediate and deep water, made by researchers over a decade ago, has led to a growing pool of accomplishments.

Included in these accomplishments are the works of Liu (1994) and Wei et al. (1995) who extended Nwogu's approach to highly nonlinear waves. This led to models that not only can be applied to intermediate water depth but also are capable of simulating wave propagation with strong nonlinear interaction. However, the nonlinear accuracy of these equations was still substantially less than the linear accuracy. Further enhancing the deep water applicability of the depth-integrated approach is the high-order Boussinesq-type equations. While the model

* Corresponding author. Fax: +1-979-862-8162.
E-mail address: plynett@civil.tamu.edu (P.J. Lynett).

0378-3839/$ - see front matter © 2004 Elsevier B.V. All rights reserved.
doi:10.1016/j.coastaleng.2004.05.004

equations described previously use a quadratic polynomial approximation for the vertical flow distribution, these high-order models use fourth- and even higher-order polynomial approximations. Gobbi et al. (2000), using a fourth-order polynomial, developed a model with excellent linear dispersive properties up to $\mu \approx 6$. Nonlinear behavior was faithfully captured to $\mu \approx 3$.

Madsen et al. (2002) developed a Boussinesq-type model, based on the method of Agnon et al. (1999), accurate to extremely deep water ($\mu \approx 40$). Their derivation, fundamentally different from the one presented in this paper, involves optimal expansions of the Laplace equation, allowing for excellent deep water linear and nonlinear dispersive properties of the resulting model. By using multiple expansions at various levels in the water column, the deep water accuracy is achieved while only requiring the fifth-order spatial derivatives found in alternative high-order models with much smaller deep water limitations. However, Madsen et al.'s model consists of more equations than the alternative high-order models, such as Gobbi et al. (2000), and thus more unknowns. Madsen et al. (2003) also presented a truncated version of the Madsen et al. (2002) model, whereby the maximum order of spatial differentiation was reduced to three, and both linear and nonlinear properties were accurate to $\mu \approx 10$.

However, all of these models employ expansions in μ and thus are still governed by the theoretical restrictions of the derivation, $\mu < 1$. On the other hand, these models have shown extensively that they are excellent prediction tools for a variety of nonlinear and deep water problems (e.g. Madsen and Schäffer, 1998; Gobbi and Kirby, 1999; Madsen et al., 2002). We need to expect some finite, although possibly very small, error in the description of wave physics for $\mu > 1$ in Boussinesq-type models, due to the small μ expansions employed. However, we can readily anticipate excellent leading-order behavior up to the "practical" limit of accuracy for a given set of equations, i.e. $\mu \approx 3$ for Nwogu's model, $\mu \approx 6$ for Gobbi et al.'s model, or $\mu \approx 40$ for Madsen et al.'s (2002) model.

Boussinesq-type modeling is founded in pragmatism; the clear and rigid fundamental limitation of the model is ignored because it is known from experience that the model yields excellent predictions beyond. This pragmatism begins to fade as the high-order models are examined. For example, the numerical scheme presented in Gobbi and Kirby (1999) to solve the model of Gobbi et al. (2000) is very lengthy, requiring the evaluation of many derivatives to an accuracy up to fifth-order. Numerical implementation of this equation system in two-horizontal dimensions would appear to be a difficult task, although certainly possible.

In this paper, a different approach to obtaining a high-order, depth-integrated model is taken. Instead of employing a high-order polynomial approximation for the vertical distribution of the flow field, N quadratic polynomials are used, matched at an interface that divides the water column into N layers. This approach leads to a set of model equations without the high-order spatial derivatives associated with high-order polynomial approximations. The multi-layer concept has been attempted previously by Kanayama et al. (1998), although the derivation and final model equations are quite different from those to be presented here. As mentioned above, Madsen et al.'s (2002) model consists of more equations than the alternative high-order models, although it is accurate into much deeper water than other models with the same order of derivatives. This is quite similar to the basic idea of the multi-layer derivation presented here: to trade fewer unknowns and higher spatial derivatives for more unknowns and lower spatial derivatives.

In the first section of this paper, the derivation of the multi-layer, depth-integrated model is presented. Analysis of the model follows, including examination of linear dispersion properties and kinematics. These properties are optimized, based on agreements with linear wave theories, and it is shown that the multi-layer model is accurate into deep water. The multi-layer equation system exhibits improvement over existing models with third-order derivatives, and can be modeled with existing numerical schemes, in both 1HD and 2HD.

2. Governing equations and boundary conditions

The goal of this derivation is to formulate a set of equations by integrating the primitive equations of motion. The integration will be performed piece-

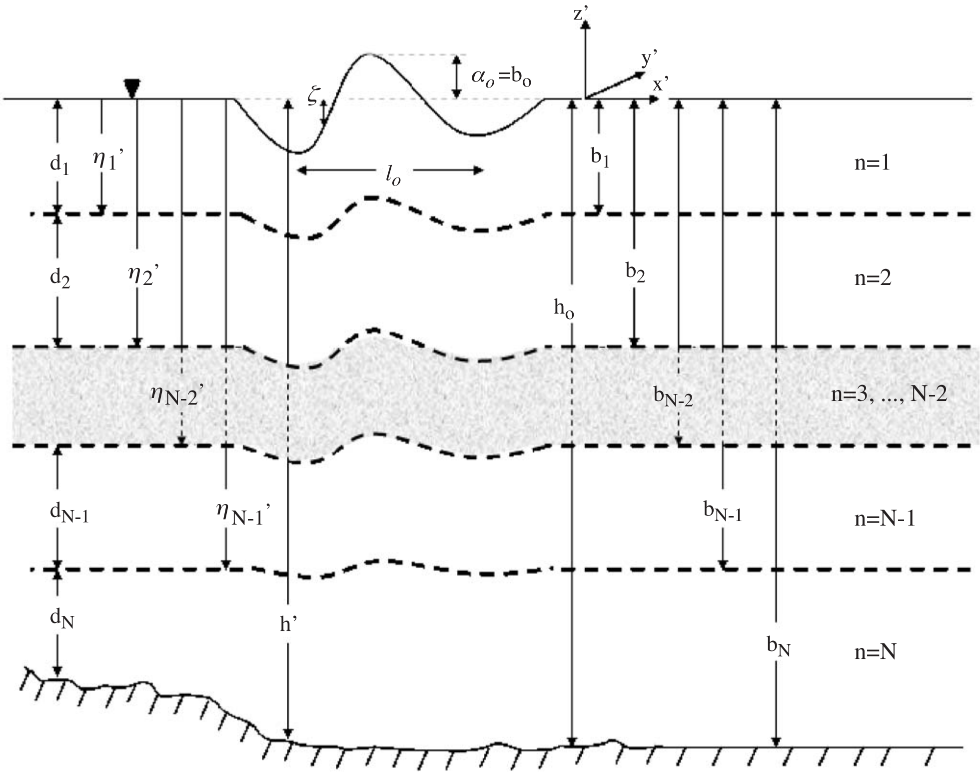

Fig. 1. N-Layer problem setup.

wisely. Note that the derivation for the specific case of the two-layer model is presented in Lynett and Liu (2004), whereas the derivation presented in this section is the general N-layer derivation.

As shown in Fig. 1, $\zeta'(x', y', t')$ denotes the free surface displacement of a wave train propagating in the water depth $h'(x', y', t')$. The boundary between layers are given as $\eta_n'(x', y', t')$. The system will be divided into N layers, where the upper and lower boundaries are given by $\eta'_o=\zeta'$ and $\eta'_N=-h'$, respectively. All of the other boundaries will be constructed as $\eta_n' = \beta_n h'$, where β_n is arbitrary and user defined. Note that h' is a function of time, and therefore so is η_n'. Each of the N layers has a characteristic thickness, d_n, as defined by Fig. 1. Utilizing the layer thicknesses d_n as the vertical length scales in the corresponding layers, h_o as the characteristic water depth, the characteristic length of the wave $\ell_o = 1/k$ as the horizontal length scale, $\ell_o/\sqrt{gh_o}$ as the time scale, and the characteristic wave amplitude a_o as the scale of wave motion, we can define the following dimensionless variables:

$$
\begin{aligned}
&(x,y) = (x',y')/\ell_o,\ z_n = z'/d_n,\ t = \sqrt{gh_o}t'/\ell_o,\\
&p_n = p_n'/\rho g a_o\ h = h'/h_o,\\
&\zeta = \zeta'/a_o, \eta_n = \eta_n'/b_n\ (U_n, V_n)\\
&\quad = (U_n', V_n')/(\varepsilon_o\sqrt{gh_o}),\ W_n = W_n'/[\varepsilon_o\mu_o\sqrt{gh_o}]
\end{aligned} \tag{1}
$$

in which the subscript n indicates the layer index, $b_o=a_o$, $b_n=\Sigma_{m=1}^{n} d_m$ for $n=1$ to N, (U_n, V_n) represents the z-dependent horizontal velocity components in the different layers, W_n the z-dependent vertical velocity component in the layers, and p_n the pressures. Note that the subscript on z indicates that the vertical coordinate is scaled differently in each layer. Dimensionless parameters have been introduced in scale, which are

$$
\varepsilon_o = a_o/h_o,\ \mu_o = h_o/\ell_o \tag{2}
$$

It is reiterated that $\ell_o = 1/k$, and thus $\mu_o = kh_o$. Assuming that the viscous effects are insignificant, the wave motion can be described by the continuity equation and the Euler's equations, i.e.

$$\frac{d_n}{h_o}\nabla\cdot\boldsymbol{U}_n + \frac{\partial W_n}{\partial z_n} = 0 \tag{3}$$

$$\frac{\partial \boldsymbol{U}_n}{\partial t} + \varepsilon_o \boldsymbol{U}_n\cdot\nabla\boldsymbol{U}_n + \varepsilon_n W_n\frac{\partial \boldsymbol{U}_n}{\partial z_n} = -\nabla p_n \tag{4}$$

$$\mu_n^2\left(\frac{\partial W_n}{\partial t} + \varepsilon_o\boldsymbol{U}_n\cdot\nabla W_n\right) + \varepsilon_o\mu_o^2 W_n\frac{\partial W_n}{\partial z_n} = -\left(\frac{\partial p_n}{\partial z_n} + \frac{1}{\varepsilon_n}\right) \tag{5}$$

where $\mu_n = d_n h_o/l_o^2$, $\varepsilon_n = a_o/d_n$, $\boldsymbol{U}_n = (U_n, V_n)$ denotes the vertically dependent horizontal velocity vector, and $\nabla = (\partial/\partial x, \partial/\partial y)$ the horizontal gradient vector.

On the free surface, $z_1 = \varepsilon_1\zeta(x, y, t)$ the usual kinematic and dynamic boundary condition applies:

$$W_1 = \frac{\partial\zeta}{\partial t} + \varepsilon_o\boldsymbol{U}_1\cdot\nabla\zeta \quad \text{on } z_1 = \varepsilon_1\zeta \tag{6}$$

$$p_1 = 0 \quad \text{on } z_1 = \varepsilon_1\zeta \tag{7}$$

Along the seafloor, $z_N = -(h_o/d_N)h$, the kinematic boundary condition requires

$$W_N + \boldsymbol{U}_N\cdot\nabla h + \frac{1}{\varepsilon_o}\frac{\partial h}{\partial t} = 0, \quad \text{on } z_N = -\frac{h_o}{d_N}h \tag{8}$$

At the imaginary interface between the layers, continuity of pressure and velocity is required:

$$p_n = p_{n+1}, \quad \text{on } z_n = \frac{b_n}{d_n}\eta_n, \quad z_{n+1} = \frac{b_n}{d_{n+1}}\eta_n \quad \text{for } n = 1 \text{ to } N-1 \tag{9}$$

$$\boldsymbol{U}_n = \boldsymbol{U}_{n+1}, \quad \text{on } z_n = \frac{b_n}{d_n}\eta_n, \quad z_{n+1} = \frac{b_n}{d_{n+1}}\eta_n \quad \text{for } n = 1 \text{ to } N-1 \tag{10}$$

$$W_n = W_{n+1}, \quad \text{on } z_n = \frac{b_n}{d_n}\eta_n, \quad z_{n+1} = \frac{b_n}{d_{n+1}}\eta_n \quad \text{for } n = 1 \text{ to } N-1 \tag{11}$$

For later use, we note here that the depth-integrated continuity equation can be obtained by integrating Eq. (3) across each of the layers. After applying the boundary conditions (Eqs. (10), (11), (6), and (8)), the resulting equation reads

$$\nabla\cdot\left[\sum_{n=1}^{N}\frac{d_n}{h_o}\int_{\frac{b_n}{d_n}\eta_n}^{\frac{b_{n-1}}{d_n}\eta_{n-1}}\boldsymbol{U}_n dz\right] + \frac{1}{\varepsilon_o}\frac{\partial h}{\partial t} + \frac{\partial\zeta}{\partial t} = 0 \tag{12}$$

We remark here that Eq. (12) is exact.

3. Approximate 2HD governing equations

A perturbation analysis will be performed utilizing the assumption

$$O(\mu_n^2) \ll 1. \tag{13}$$

Using μ_n^2 as the small parameter, we can expand the dimensionless physical variables as power series of μ_n^2

$$f = \sum_{M=0}^{\infty}\mu_n^{2M} f^{[M]}; \quad (f = \boldsymbol{U}_n, W_n, \zeta, p_n) \tag{14}$$

Furthermore, we will adopt the irrotational assumption, yielding the following conditions

$$\frac{\partial}{\partial z_n}\boldsymbol{U}_n^{[0]} = 0, \tag{15}$$

$$\frac{\partial}{\partial z_n}\boldsymbol{U}_n^{[1]} = \nabla W_n^{[0]}. \tag{16}$$

Consequently, from Eq. (15), the leading order horizontal velocity components are independent of the vertical coordinate, i.e.,

$$\boldsymbol{U}_n^{[0]} = \boldsymbol{U}_n^{[0]}(x, y, t). \tag{17}$$

Substituting Eq. (14) into the continuity equation (3) and the boundary conditions (6) and (8), we collect the leading order terms as

$$\frac{d_n}{h_o}\nabla\cdot\boldsymbol{U}_n^{[0]}+\frac{\partial W_n^{[0]}}{\partial z_n}=0 \quad \text{for } n=1 \text{ to } N-1 \tag{18}$$

$$W_1^{[0]}=\frac{\partial\zeta}{\partial t}+\varepsilon_o\boldsymbol{U}_1^{[0]}\cdot\nabla\zeta \quad \text{on } z_1=\varepsilon_1\zeta \tag{19}$$

$$W_N^{[0]}+\boldsymbol{U}_N^{[0]}\cdot\nabla h+\frac{1}{\varepsilon_o}\frac{\partial h}{\partial t}=0 \quad \text{on } z_N=-\frac{h_o}{d_N}h \tag{20}$$

Integrating Eq. (18) with respect to z_n and using Eqs. (11) and (20) to determine the integration constants, we obtain the vertical profile of the vertical velocity components in the layers:

$$W_n^{[0]}=-z_nS_n^{[0]}-T_n^{[0]} \tag{21}$$

where

$$S_n^{[0]}=\frac{d_n}{h_o}\nabla\cdot\mathbf{U}_n^{[0]}$$

$$T_n^{[0]}=\sum_{m=n}^{N-1}\eta_m\left(\frac{b_m}{d_{m+1}}S_{m+1}^{[0]}-\frac{b_m}{d_m}S_m^{[0]}\right)+\nabla\cdot(h\mathbf{U}_N^{[0]})+\frac{1}{\varepsilon_o}\frac{\partial h}{\partial t} \tag{22}$$

Similarly, integrating Eq. (16) with respect to z with information from Eq. (21), we can find the corresponding vertical profiles of the horizontal velocity components:

$$\boldsymbol{U}_n^{[1]}=-\frac{z_n^2}{2}S_n^{[0]}-z_n\nabla T_n^{[0]}+\boldsymbol{C}_n(x,y,t) \tag{23}$$

in which $\boldsymbol{C}_n$ are unknown functions. Up to $O(\mu_n^2)$, the horizontal velocity components can be expressed as

$$\boldsymbol{U}_n=\boldsymbol{U}_n^{[0]}(x,y,t)+\mu_n^2\boldsymbol{U}_n^{[1]}(x,y,z,t)+O(\mu_n^4) \tag{24}$$

Now, we can define the horizontal velocity vectors, $\boldsymbol{u}_n$ $(x, y, \kappa_n(x, y, t), t)$ evaluated at $z=\kappa_n$ (x, y, t) as

$$\boldsymbol{u}_n=\boldsymbol{U}_n^{[0]}-\mu_n^2\{\mathcal{A}_n\nabla S_n^{[0]}+\mathcal{B}_n\nabla T_n^{[0]}+\boldsymbol{C}_n\}+O(\mu_n^4) \tag{25}$$

where $\mathcal{A}_n=\kappa_n^2/2$ and $\mathcal{B}_n=\kappa_n$. The above substitution follows the method of Nwogu (1993), and leads to an "extended" set of multi-layer equations. One could also layer-average (Eq. (24)), which would then lead to the "conventional" set of depth-averaged multi-layer equations. Layer-averaging (Eq. (24)) yields the same form as Eq. (25), but with $\mathcal{A}_n=1/6(\eta_{n-1}^2+\eta_{n-1}\eta_n+\eta_n^2)$ and $\mathcal{B}_n=1/2(\eta_{n-1}+\eta_n)$. Thus we can continue the derivation, while keeping in mind it is valid for both "extended" and depth-averaged approaches.

Subtracting Eq. (25) from Eq. (24), we can express $\boldsymbol{U}_n$ in terms of $\boldsymbol{u}_n$ as

$$\boldsymbol{U}_n=\boldsymbol{u}_n-\mu_n^2\left\{\left(\frac{z^2}{2}-\mathcal{A}_n\right)\nabla S_n+(z-\mathcal{B}_n)\nabla T_n\right\}+O(\mu_n^4) \tag{26}$$

where

$$S_n=\frac{d_n}{h_o}\nabla\cdot\boldsymbol{u}_n$$

$$T_n=\sum_{m=n}^{N-1}\eta_n\left(\frac{b_m}{d_{m+1}}S_{m+1}-\frac{b_m}{d_m}S_m\right)+\nabla\cdot(h\boldsymbol{u}_N)+\frac{1}{\varepsilon_o}\frac{\partial h}{\partial t} \tag{27}$$

The exact continuity equation (12) can be rewritten approximately in terms of ζ and $\boldsymbol{u}_n$. Substituting Eq. (26) into Eq. (12), we obtain

$$\frac{1}{\varepsilon_o}\frac{\partial h}{\partial t}+\frac{\partial\zeta}{\partial t}+\nabla\cdot\sum_{n=1}^{N}\left(\frac{b_{n-1}}{h_o}\eta_{n-1}-\frac{b_n}{h_o}\eta_n\right)\boldsymbol{u}_n$$
$$-\nabla\cdot\sum_{n=1}^{N}\mu_n^2\frac{d_n}{h_o}\left\{\left[\frac{\left(\frac{b_{n-1}}{d_n}\eta_{n-1}\right)^3-\left(\frac{b_n}{d_n}\eta_n\right)^3}{6}-\left(\frac{b_{n-1}}{d_n}\eta_{n-1}-\frac{b_n}{d_n}\eta_n\right)\mathcal{A}_n\right]\nabla S_n\right.$$
$$\left.+\left[\frac{\left(\frac{b_{n-1}}{d_n}\eta_{n-1}\right)^2-\left(\frac{b_n}{d_n}\eta_n\right)^2}{2}-\left(\frac{b_{n-1}}{d_n}\eta_{n-1}-\frac{b_n}{d_n}\eta_n\right)\mathcal{B}_n\right]\nabla T_n\right\}=O(\mu_n^4) \tag{28}$$

Note that all the dispersive (μ) terms disappear for the depth-averaged formulation; this can also be shown by substituting the integral definitions of the depth-averaged velocities into Eq. (12). Eq. (28) is one of three governing equations for ζ and $\boldsymbol{u}_n$. The other two equations come from the horizontal momentum equation (4). However, we must find the pressure field first. This can be accomplished by approximating the vertical momentum equation (5) as

$$\frac{\partial p_n}{\partial z_n} = -\frac{1}{\varepsilon_n} - \mu_n^2\left(\frac{\partial W_n^{[0]}}{\partial t} + \varepsilon_o \boldsymbol{U}_n^{[0]} \cdot \nabla W_n^{[0]}\right) - \mu_0^2\left(\varepsilon_o W_n^{[0]}\frac{\partial W_n^{[0]}}{\partial z_n}\right) + O(\mu_0^2\mu_n^2, \mu_n^4) \tag{29}$$

We can integrate the equation above with respect to z_1 to find the pressure field in the upper layer as

$$\begin{aligned} p_1 = {} & \left(\zeta - \frac{z_1}{\varepsilon_1}\right) + \mu_1^2\left\{\frac{1}{2}(z_1^2 - \varepsilon_1^2\zeta^2)\frac{\partial S_1}{\partial t}\right. \\ & + (z_1 - \varepsilon_1\zeta)\frac{\partial T_1}{\partial t} + \frac{\varepsilon_o}{2}(z_1^2 - \varepsilon_1^2\zeta^2)\boldsymbol{u}_1 \cdot \nabla S_1 \\ & \left. + \varepsilon_o(z_1 - \varepsilon_1\zeta)\boldsymbol{u}_1 \cdot \nabla T_1\right\} \\ & + \varepsilon_o\mu_0^2\left\{\frac{1}{2}(\varepsilon_1^2\zeta^2 - z_1^2)S_1^2 + (\varepsilon_1\zeta - z_1)S_1T_1\right\} \\ & + O(\mu_o^2\mu_1^2), \eta_1 < z_1 < \varepsilon_1\zeta \end{aligned} \tag{30}$$

To derive the governing equations for $\boldsymbol{u}_1$, we substitute Eqs. (26) and (30) into Eq. (4), enforce zero vertical vorticity (see Hsiao and Liu, 2002), and obtain the following equation,

$$\begin{aligned} & \frac{\partial \boldsymbol{u}_1}{\partial t} + \frac{\varepsilon_o}{2}\nabla(\boldsymbol{u}_1 \cdot \boldsymbol{u}_1) + \nabla\zeta + \mu_1^2\frac{\partial}{\partial t}\{\mathcal{A}_1\nabla S_1 \\ & + \mathcal{B}_1\nabla T_1\} + \varepsilon_o\mu_1^2\nabla(\mathcal{B}_1\boldsymbol{u}_1 \cdot \nabla T_1 + \mathcal{A}_1\boldsymbol{u}_1 \cdot \nabla S_1) \\ & + \varepsilon_o\mu_o^2\left[T_1\nabla T_1 - \nabla\left(\zeta\frac{\partial T_1}{\partial T}\right)\right] \\ & + \varepsilon_o^2\mu_o^2\nabla\left(\zeta S_1T_1 - \frac{h_o}{d_1}\frac{\zeta^2}{2}\frac{\partial S_1}{\partial t} - \zeta\boldsymbol{u}_1 \cdot \nabla T_1\right) \\ & + \varepsilon_o^2\varepsilon_1\mu_o^2\nabla\left[\frac{\zeta^2}{2}\left(S_1^2 - \frac{h_o}{d_1}\boldsymbol{u}_1 \cdot \nabla S_1\right)\right] = O(\mu_o^2\mu_1^2) \end{aligned} \tag{31}$$

It is remarked here that $\varepsilon_o\mu_o^2 = \varepsilon_1\mu_1^2$, and all coefficients are written in terms of μ_o and ε_o whenever possible. Determination of $\boldsymbol{u}_n$ for $n=2$ to N does not require solving additional momentum equations. With boundary condition (10) and the known velocity profiles (Eq. (26)), $\boldsymbol{u}_n$ can be given as a function of $\boldsymbol{u}_{n-1}$:

$$\begin{aligned} & \boldsymbol{u}_n + \mu_n^2\left\{\left[\mathcal{A}_n - \frac{\left(\frac{b_{n-1}}{d_n}\eta_{n-1}\right)^2}{2}\right]\nabla S_n + \left(\mathcal{B}_n - \frac{b_{n-1}}{d_n}\eta_{n-1}\right)\nabla T_n\right\} \\ & = \boldsymbol{u}_{n-1} + \mu_{n-1}^2\left\{\left[\mathcal{A}_{n-1} - \frac{\left(\frac{b_{n-1}}{d_{n-1}}\eta_{n-1}\right)^2}{2}\right]\nabla S_{n-1} + \left(\mathcal{B}_{n-1} - \frac{b_{n-1}}{d_{n-1}}\eta_{n-1}\right)\nabla T_{n-1}\right\} + O(\mu_{n-1}^4, \mu_n^4) \end{aligned} \tag{32}$$

Thus, the lower layer velocities can be directly calculated with knowledge of the upper layer velocity. Eqs. (28), (31), and (32) are the coupled governing equations, written in terms of $\boldsymbol{u}_n$ and ζ, for highly nonlinear, dispersive waves. To complete the boundary value problem and solve the above system of equations, an initial condition for $\boldsymbol{u}_n$ and ζ is required, as are spatial boundary conditions. For a vertical wall, the stable numerical procedure given by Kirby et al. (1998), i.e. for a wall with a normal vector in the x-direction:

$$u_n = \frac{\partial \zeta}{\partial x} = \frac{\partial v_n}{\partial x} = 0 \tag{33}$$

should be followed.

A question that arises with the use of the matched velocity profiles in each layer is whether the vertical velocity gradients are continuous across the layer boundary, which is not a directly enforced boundary condition. If the gradients are not continuous, there is a discontinuity of the nonlinear, vertical transport terms in the horizontal and vertical Euler's equations.

Specifically, the discontinuity would arise in the $W_n(\partial \boldsymbol{U}_n/\partial z_n)$ term in Eq. (4) and the $\mu_o^2 W_n(\partial W_n/\partial z_n)$ term in Eq. (5). However, with calculation of these nonlinear terms using the derived vertical velocity profiles, Eq. (21), and horizontal velocity profiles, Eq. (26), it can readily be shown that the discontinuity is of the truncation error order in the final model, i.e.

$$\frac{\partial \boldsymbol{U}_n\left(z_n = \frac{b_n}{d_n}\eta_n\right)}{\partial z_n} = \frac{\partial \boldsymbol{U}_{n+1}\left(z_{n+1} = \frac{b_n}{d_{n+1}}\eta_n\right)}{\partial z_{n+1}} + O(\mu_n^4, \mu_{n+1}^4) \quad (34)$$

$$\mu_o^2\frac{\partial W_n\left(z_n = \frac{b_n}{d_n}\eta_n\right)}{\partial z_n} = \mu_o^2\frac{\partial W_{n+1}\left(z_{n+1} = \frac{b_n}{d_{n+1}}\eta_n\right)}{\partial z_{n+1}} + O(\mu_o^2\mu_n^2, \mu_o^2\mu_{n+1}^2) \quad (35)$$

Therefore, the discontinuity of the nonlinear, vertical transport terms will not affect the overall accuracy of the model. An important consequence of this statement is that to the derived order of accuracy of the model all of the individual velocities, $\boldsymbol{u}_n$, exist on the same quadratic velocity profile. It is simple exercise to explicitly show this; with μ_n^2 manipulations in Eq. (24), all $\boldsymbol{U}_n$ can be reduced to an identical expression. At this point, the pragmatism aspect of Boussinesq-type modeling takes over this paper. It will be shown in the next section that the multi-layering approach yields significant benefits beyond the derived order of accuracy of the model, which has been the focus of Boussinesq-type modeling since Madsen and Sorensen (1992) and Nwogu (1993).

4. Accuracy of multi-layer model

4.1. Dispersion relation

In this section, the accuracy of the multi-layer linear dispersion properties, namely phase and group velocity, will be examined. First, let us define the arbitrary evaluation levels and the boundary between the two layers as:

$$\kappa_n = \alpha_n h, \qquad \eta_n = \beta_n h \quad (36)$$

where the coefficients α and β are arbitrary and to be defined. The dispersion relation is determined by first truncating all nonlinear and depth-variable terms from Eqs. (28), (31), and (32). Then the assumed solution forms

$$\zeta = \zeta^{(0)} e^{i\theta} \quad \boldsymbol{u}_n = \boldsymbol{u}_n^{(0)} e^{i\theta}, \quad (37)$$

where $\theta = kx - wt$, k is the wave number, and w is the wave frequency, are substituted into the reduced governing equations. Finding the dispersion relation follows straightforwardly, although the algebra becomes tedious as the number of layers increases. The symbolic math program Mathematica was used to check all calculations. The dispersion relations for a number of the models are included in Appendix A, those not included are extremely lengthy expressions and can be obtained from the first author.

It should be noted that when analyzing the "extended" (EXT) form of the multi-layer equations, the dispersion relation takes the general form:

$$\frac{w^2}{k^2 gh} = \frac{1 + (kh)^2 N_1 + \ldots + (kh)^{2N} N_N}{1 + (kh)^2 D_1 + \ldots + (kh)^{2N} D_N} \quad (38)$$

where N and D are coefficients which are functions of the α and β values. Eq. (38) demonstrates that for the extended form, the maximum powers of kh are the same in both numerator and denominator, and the highest of these powers is equal to $2N$, where N is the number of layers used. When looking at the "depth-averaged" (DA) form of the multi-layer equations, the dispersion relation becomes

$$\frac{w^2}{k^2 gh} = \frac{1 + (kh)^2 N_1 + \ldots + (kh)^{2(N-1)} N_{N-1}}{1 + (kh)^2 D_1 + \ldots + (kh)^{2N} D_N} \quad (39)$$

where N and D are functions of only the β values. Now the maximum powers of kh in the numerator and denominator do not match, with the numerator containing a power of two less. This property will lead to very different degrees of accuracy when comparing the extended and conventional approaches.

Defining a model accuracy, or model error, can be difficult and often can depend on the specific physical problem being examined. For this analysis, a representation of the overall error including errors in wave speed and group velocity is sought. The error will be given by the minimization parameter Δ_{Linear}:

$$\Delta_{\mathrm{Linear}} = \frac{1}{2} \times \left(\frac{\sum_{kh=0.1}^{\Omega} \frac{|c^{\mathrm{e}} - c|}{kh}}{\sum_{kh=0.1}^{\Omega} \frac{|c^{\mathrm{e}}|}{kh}} + \frac{\sum_{kh=0.1}^{\Omega} \frac{|c_{\mathrm{g}}^{\mathrm{e}} - c_{\mathrm{g}}|}{kh}}{\sum_{kh=0.1}^{\Omega} \frac{|c_{\mathrm{g}}^{\mathrm{e}}|}{kh}} \right) \tag{40}$$

where c^{e} and $c_{\mathrm{g}}^{\mathrm{e}}$ are the exact linear phase speed and group velocity, whereas c and c_{g} are the approximate values taken from the multi-layer model derived here. The right-hand side is divided by two, so as to normalize the total error created by the two different sources. All of the summations are divided by kh so that errors at low wave numbers are more important than high wave number errors. The reason for this weighting is a peculiarity of the optimization: it was possible to sacrifice low wave number accuracy for accuracy at higher wave numbers. Accuracy at low wave numbers is paramount for this shallow water based model, and hence the weighting. Summations are started at $kh = 0.1$ also because of the kh weighting, and the subsequent need to avoid division by zero. The upper summation limit, $kh = \Omega$, is determined such that the minimum Δ_{Linear} is less than some threshold. For all of the optimizations presented here, Ω is determined such that Δ_{Linear} lies between 0.001 and 0.002. This small range is used, rather than an exact number, due to the computational requirements of optimizing the large number of layer models to high coefficient precision.

Table 1
Optimization results for "extended" multi-layer model

	1-L EXT	2-L EXT	3-L EXT	4-L EXT
α_1	−0.531	−0.200	−0.1050	−0.0600
β_1		−0.376	−0.1965	−0.1125
α_2		−0.680	−0.3675	−0.2200
β_2			−0.5550	−0.3400
α_3			−0.7875	−0.5165
β_3				−0.7000
α_4				−0.8800
$\Omega(kh)$	3	6	12	18

Note that the three- and four-layer levels were determined in increments of 0.0005.

Table 2
Optimization results for depth-averaged multi-layer model

	2-L DA	3-L DA	4-L DA	5-L DA
β_1	−0.332	−0.180	−0.114	−0.076
β_2		−0.447	−0.269	−0.167
β_3			−0.505	−0.290
β_4				−0.510
β_5				
$\Omega(kh)$	2	3	4	5

Tables 1 and 2 summarize the optimization results for the EXT and DA models, respectively. Note that with the use of Eq. (40) and $\Omega = 3$, the best fit α_1 for the one-layer model is -0.531, which is the exact value recommended by Nwogu (1993). Figs. 2 and 3 plot the errors in phase and group velocity for the various different models.

Perhaps the most striking feature of these plots is clear in Fig. 3, the phase and group velocity errors for the DA formulation. While the magnitude of the errors certainly does decrease with increasing number of layers, there are reasonably large errors starting at $kh \approx 1$ regardless of the number of layers employed. The phenomenon is due to the properties of the dispersion relation for the DA formulation, which simply cannot be manipulated to yield close agreement with the tanh function for $kh > 1$. The easiest demonstration of this deficiency is to show that it is impossible to force the coefficients in the DA dispersion relation to match a Padè approximation. Looking back to Eq. (39), the coefficient N_1 for the two-layer DA model is $-1/3(\beta_1 + \beta_1^2)$. The same-power coefficient in the [2,4] Padè approximation of $\tanh(kh)/kh$ is 2/21. N_1 can never be equal to 2/21 in the real number domain, and thus it is impossible for the two-layer DA model to match a Padè approximation. This fact is evidence that the DA multi-layer formulation will not exhibit significant practical gains over the single-layer models.

On the other hand, the EXT formulation shows great promise of application into very deep water. From Fig. 2, it can be seen that increasing the number of layers within the EXT formulation increases the deep water accuracy significantly, with the four-layer model exhibiting a 1% phase error at $kh \approx 30$. Also

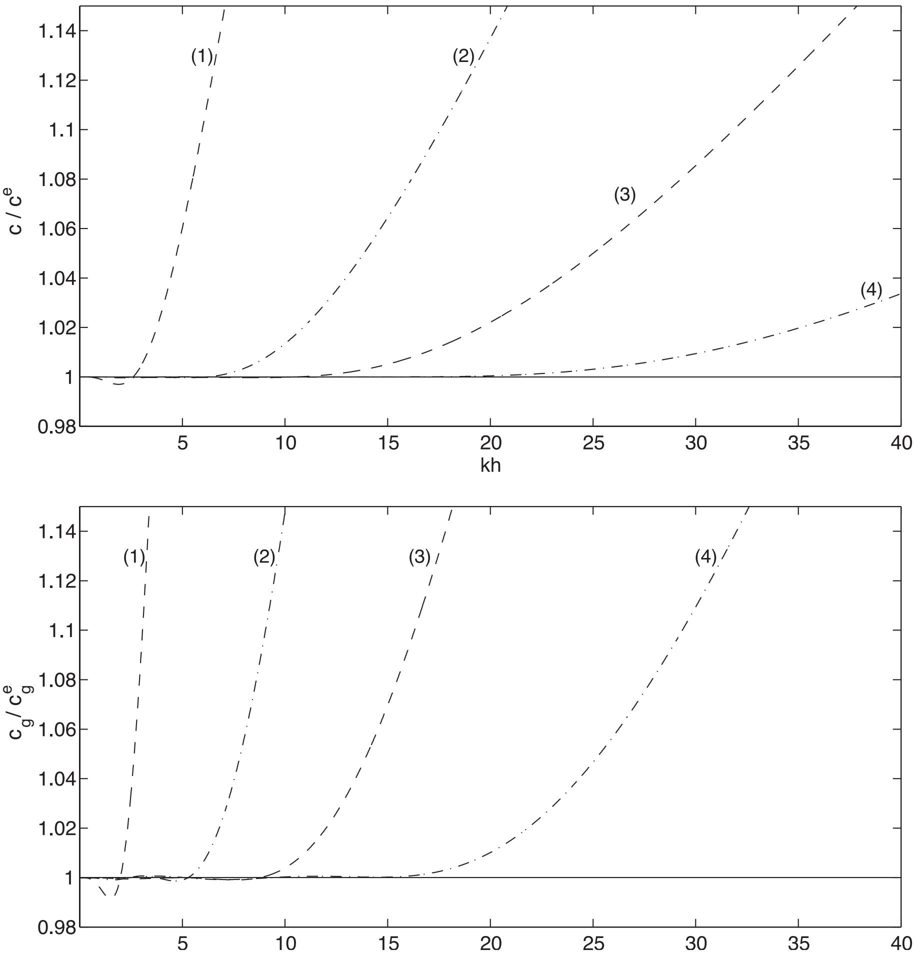

Fig. 2. Comparison of wave speed and group velocity for the extended multi-layer model. Curve (1) is the one-layer model of Nwogu, (2) is the two-layer model, (3) is the three-layer model, and (4) is the four-layer model.

note that, as is common with Boussinesq-type equations, the group velocity error is larger than the celerity error.

At this point in this paper, the DA formulation will no longer be discussed. Acceptable DA dispersion relation accuracy cannot be achieved for $kh>1$, and thus further analysis of the DA model is largely without practical purpose. The small increase in deep water accuracy due to increasing the number of layers does not justify the additional computational requirements. From here on, all analysis will examine the EXT model. As a side note, due to the fact that there are N same-order unknowns in the N-layer derivation (i.e. $\boldsymbol{U}_1^{[0]}$, $\boldsymbol{U}_2^{[0]}, \ldots$), the model is particularly flexible in terms of $O(\mu_n^2)$ substitutions. Therefore, it may be possible to manipulate the DA formulation in order to achieve better linear dispersion properties, although this comes at the cost of altering the fundamental physics of the derivation.

4.2. Velocity profiles

The vertical profiles of both horizontal and vertical velocity can be readily obtained from Eqs. (21) and (26), respectively. Let us define the function $f_u(z)$ as the horizontal velocity, normalized by the velocity at $z=0$, of a monochromatic wave propagating over a

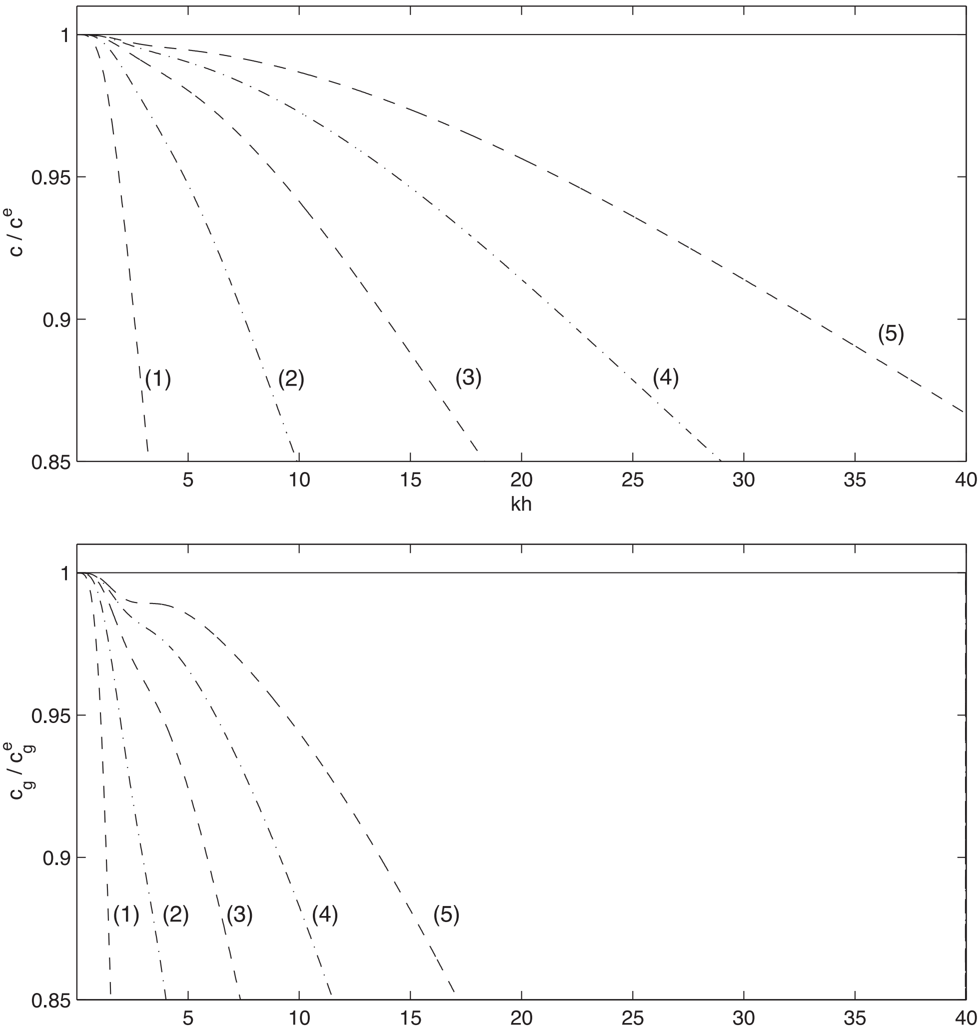

Fig. 3. Comparison of wave speed and group velocity for the depth-averaged multi-layer model. Curve (1) is the one-layer model of Peregrine, (2) is the two-layer model, (3) is the three-layer model, (4) is the four-layer model, and (5) is the five-layer model.

constant depth. This function is composed of N quadratic polynomial elements, given by:

$$f_u(z) = f_u(\eta_{n-1}) \times \frac{1 + (kh)^2\left[\frac{1}{2}\left(\frac{z^2}{h^2} - \alpha_n^2\right) + \left(\alpha_n - \frac{z}{h}\right)\Pi_n\right]}{1 + (kh)^2\left[\frac{1}{2}\left(\beta_{n-1}^2 - \alpha_n^2\right) + (\alpha_n - \beta_{n-1})\Pi_n\right]}$$

$$\text{for } \beta_{n-1}h = \eta_{n-1} \geq z \geq \eta_n = \beta_n h \text{ and } n = 1, N \quad (41)$$

where

$$\Pi_n = \beta_n - \sum_{m=n+1}^{N} \frac{u_m^{(0)}}{u_n^{(0)}}(\beta_{m-1} - \beta_m) \quad (42)$$

The reader should keep in mind that $\beta_0 = 0$, corresponding to the free surface, $\beta_N = -1$, corresponding to the seafloor, and $f_u(0) = 1$. From the linear equation systems, after the substitutions of Eq. (37), there can be derived explicit expressions for $u_n^{(0)}$, and thus the velocity ratios can be evaluated.

Similarly, the vertical velocity profile, normalized by the velocity at the still water level, is given by $f_w(z)$

$$f_w(z) = f_w(\eta_{n-1}) \frac{\frac{z}{h} - \Pi_n}{\beta_{n-1} - \Pi_n} \text{ for } \beta_{n-1}h = \eta_{n-1} \geq z \geq \eta_n = \beta_n h \text{ and } n = 1, N \quad (43)$$

which is a piecewise linear function. Note that, as with f_u, $f_w(0)=1$.

Figs. 4–7 show the kinematics comparisons for the one-, two-, three- and four-layer models. Fig. 4 gives the comparisons for $kh=\pi$. Even for the one-layer model, whose practical accuracy has been demonstrated repeatedly, there are large errors on both the u and w vertical profiles. There is some small error in the two-layer model, but the three- and four-layer models predict the vertical profiles to a very high degree of accuracy. For $kh=2\pi$, shown in Fig. 5, the two-layer model is still very accurate, although errors in the w profile are becoming significant. Moving into deeper water, Fig. 6, for

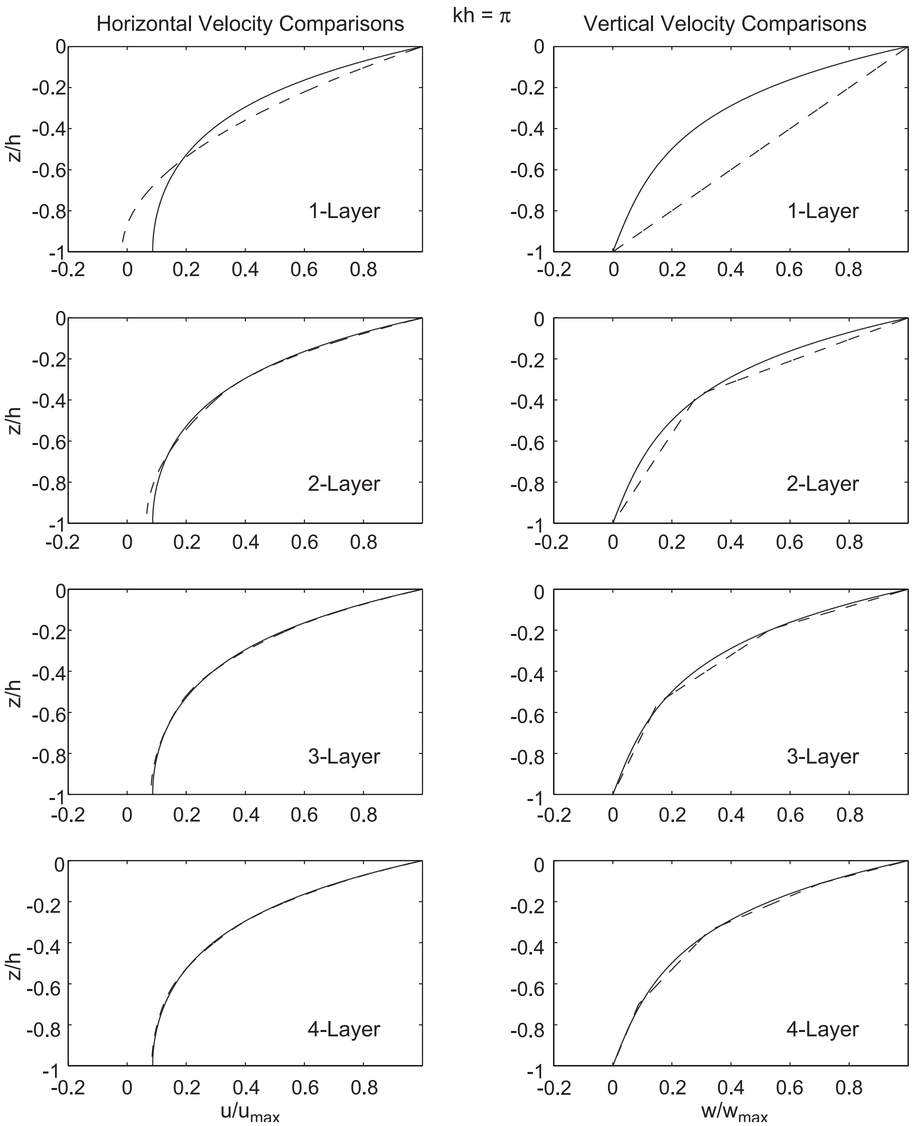

Fig. 4. Comparison of vertical profiles of horizontal (left column) and vertical (right column) velocity for $kh=\pi$. The profiles from linear theory are given by the solid lines and the dashed by the multi-layer theory, where the first row is the one-layer (extended Boussinesq) model, the second row is the two-layer, the third row is the three-layer, and fourth row is the four-layer.

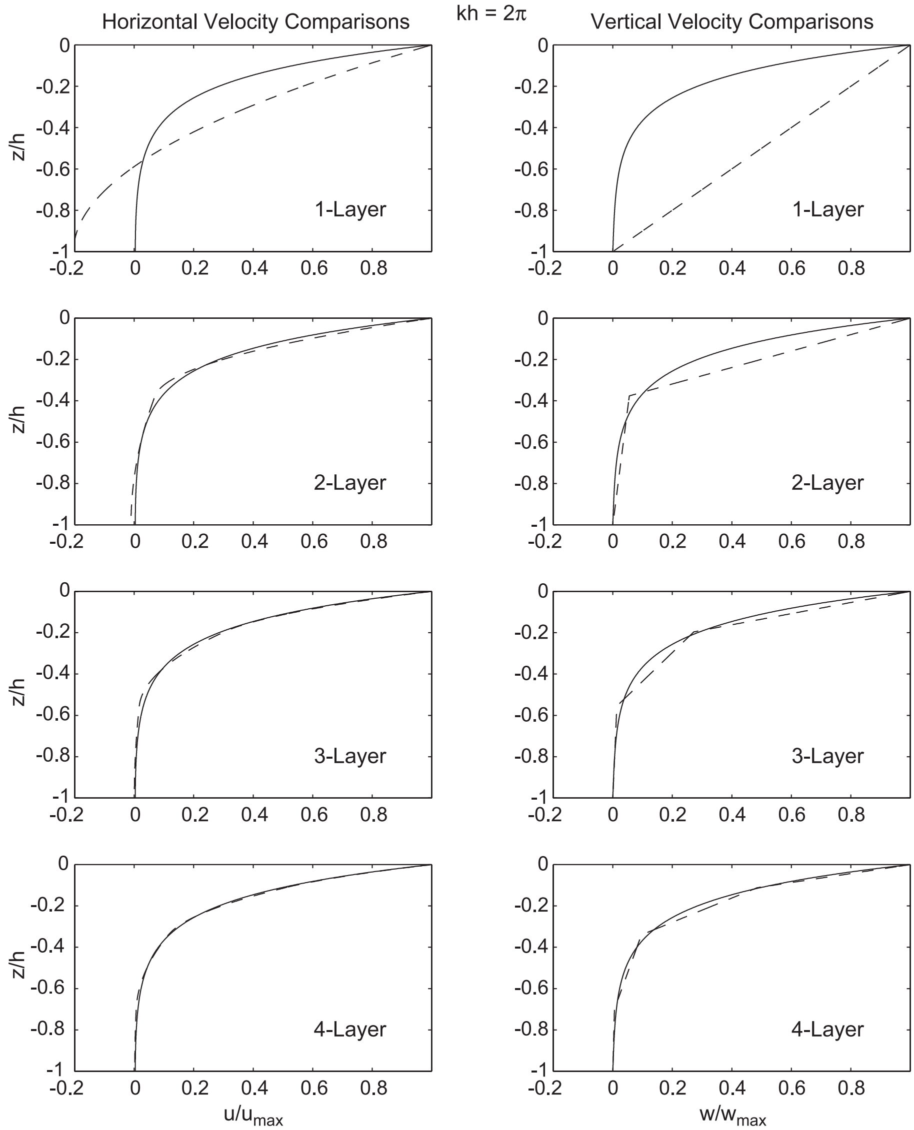

Fig. 5. Comparison of vertical profiles of horizontal (left column) and vertical (right column) velocity for $kh=2\pi$. Figure setup is the same as in Fig. 4.

$kh=4\pi$, illustrates the accuracy of the three- and four-layer models. Even into extremely deep water, the four-layer model is more than adequate, as displayed in Fig. 7 for $kh=8\pi$. Note that presenting the vertical profiles from the one-layer into this kh range is done only for consistency among the figures. While one can use Figs. 4–7 to understand the vertical flexibility of the various models, the errors in the magnitude of the velocities must also be considered, which are similar to the errors in phase velocity.

4.3. Comparisons with other Boussinesq-type models

As there are a number of high-order, Boussinesq-like approaches in the published literature, it is important to discuss how the multi-layer model compares. In an attempt to discriminate the advantages

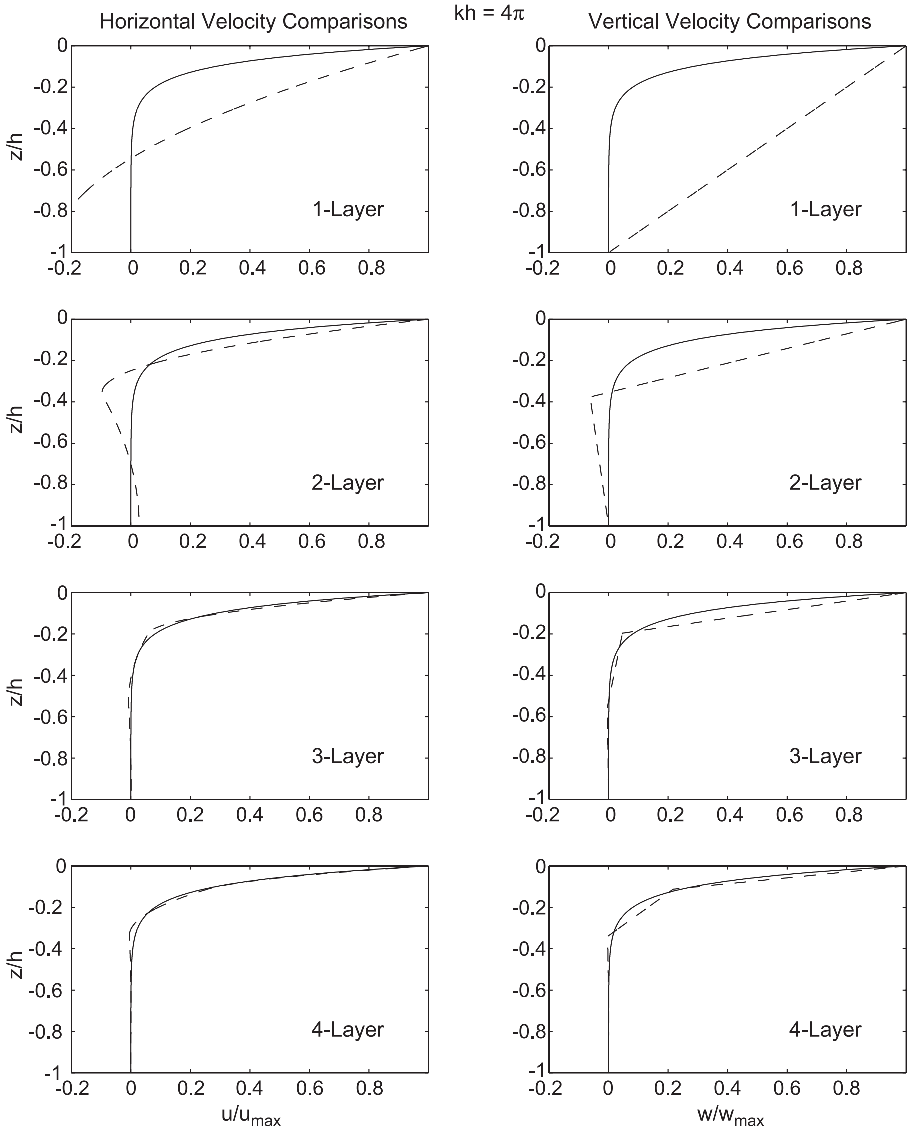

Fig. 6. Comparison of vertical profiles of horizontal (left column) and vertical (right column) velocity for $kh=4\pi$. Figure setup is the same as in Fig. 4.

and disadvantages of the various models, four items are compared: kh at 1% error in phase speed, number of equations, number of vector equations, and highest order of spatial differentiation. These items are given in Table 3.

All of the values shown in Table 3 are taken directly from the corresponding papers. For Madsen et al. (2002), results given above are for their $\sigma=-0.2$ and Eqs. (2), (15), (17, and (22b). For Madsen et al. (2003), results given above are for $\sigma=-0.5$, given in Table 2 in their appendix. The equations for Madsen et al. (2003) are similar to Madsen et al. (2002), except with all derivatives higher than third-order truncated. The two-layer model has slightly better linear dispersion accuracy than Schäffer and Madsen and Gobbi et al., but

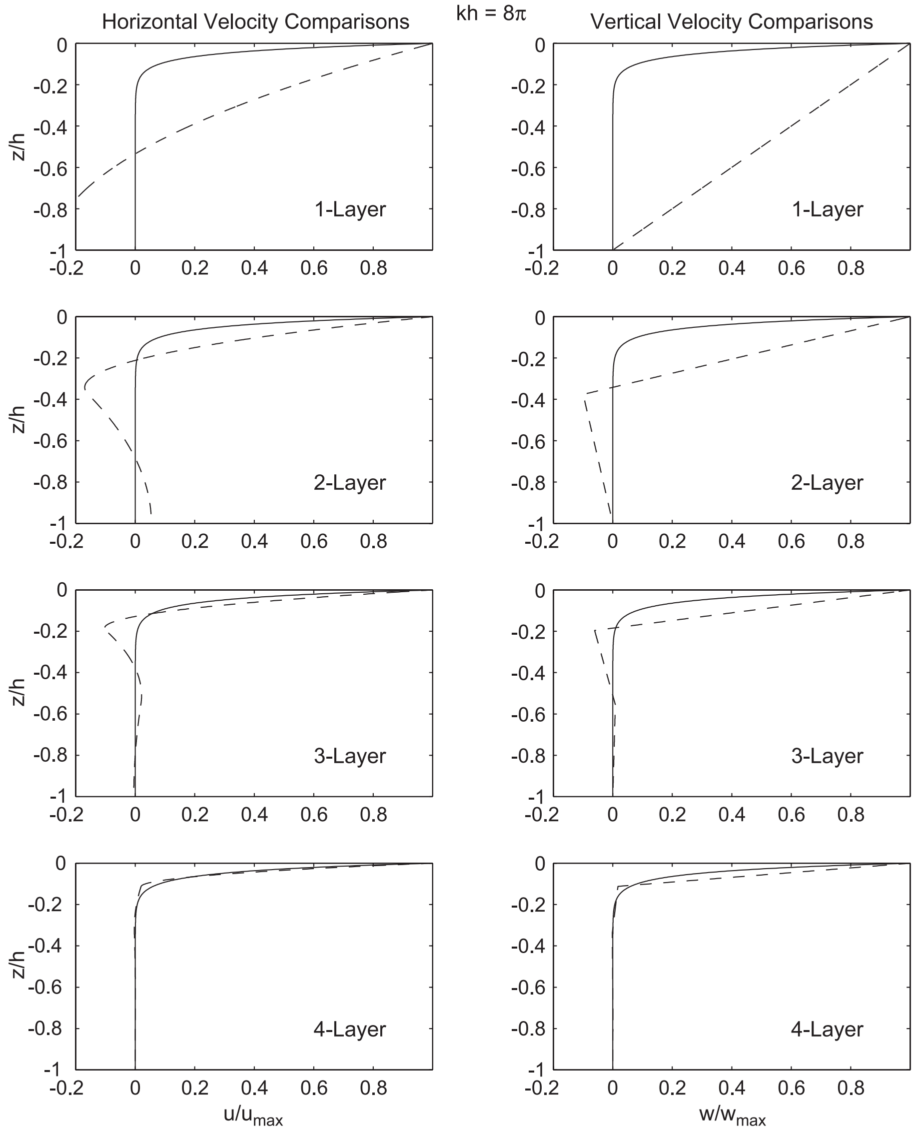

Fig. 7. Comparison of vertical profiles of horizontal (left column) and vertical (right column) velocity for $kh = 8\pi$. Figure setup is the same as in Fig. 4.

slightly worse than Madsen et al. (2003). The accuracy of the four-layer model is approaching that of Madsen et al. (2002), but is still substantially below. The computational requirements of Madsen et al. (2003) and the four-layer model would probably be very similar, as they both include only third order derivatives, and consist of identical numbers of equations for a 2HD problem. Of course, the method of numerical solving can greatly affect these judgements.

5. Conclusions

A model for the transformation of highly dispersive waves is derived. The model utilizes N quadratic

Table 3
Comparison of different aspects of the high-order models of Schäffer and Madsen (1995) with truncation error $[O(\varepsilon_o\mu_o^2, \mu_o^4)]$, Gobbi et al. (2000) $[O(\mu_o^6)]$, Madsen et al. (2002) $[O(\mu_o^{10})]$, Madsen et al. (2003) $[O(\mu_o^6)]$, and the two-, three-, and four-layer model presented here $[O(\mu_o^2\mu_1^2, \mu_N^4)]$

Model	kh at 1% error in c
Schäffer and Madsen (1995)	6
Gobbi et al. (2000)	6
Madsen et al. (2002)	40
Madsen et al. (2003)	10
Two-layer	8
Three-layer	17
Four-layer	30

Model	# of equation [# of vector equations] (differentiation order)
Schäffer and Madsen (1995)	2 [1] (3)
Gobbi et al. (2000)	2 [1] (5)
Madsen et al. (2002)	6 [3] (5)
Madsen et al. (2003)	6 [3] (3)
Two-layer	3 [2] (3)
Three-layer	4 [3] (3)
Four-layer	5 [4] (3)

polynomials to approximate the vertical flow field, matched along an interface. Through optimization of the interface and velocity evaluation locations, it is shown that the two-layer model exhibits accurate characteristics up to a $kh \approx 8$. The three- and four-layer models show accuracy into even deeper water, while also including only third-order spatial derivatives. Owing to this maximum order of differentiation, a tractable numerical algorithm can be developed for the general 2HD problem, employing the well-studied predictor–corrector scheme (e.g. Wei et al., 1995). The multi-layer model represents an extension of the practical-oriented Boussinesq developments of a decade ago, allowing for high-order accuracy with a relatively simple set of 2HD model equations.

To employ the multi-layer model in real world situations, shoreline conditions and parameterizations of viscous effects must be included. While implementations of the existing models, e.g. the roller model for breaking, can be readily integrated into the multi-layer framework, it may be possible to enhance these previous foundations, by, for example, including the effects of vertically dependent eddy viscosities. Extensions such as this are currently being explored within the multi-layer framework.

Acknowledgements

The research reported here is partially supported by Grants from National Science Foundation (CMS-9528013, CTS-9808542, and CMS-9908392).

Appendix A. Dispersion relation coefficients

The general form of the dispersion relation for the N-layer model can be given as

$$\frac{w^2}{k^2gh} = \frac{1 + (kh)^2 N_1 + \ldots + (kh)^{2N} N_N}{1 + (kh)^2 D_1 + \ldots + (kh)^{2N} D_N}. \tag{44}$$

Where space permits, the function form of the coefficients N and D are given below. Where the expressions are tedious, only the numerical values of the coefficients are given, using the α and β values included in Tables 1 and 2.

A.1. EXT Formulation

A.1.1. One-layer model

$N_1 = -1/3 - 1/2\alpha_1^2 - \alpha_1$
$D_1 = -1/2\alpha_1^2 - \alpha_1$

A.1.2. Two-layer model

$N_1 = \delta_2\delta_7 - \delta_1\delta_8 - \delta_3 - \delta_4$
$N_2 = \delta_3\delta_8 - \delta_4\delta_7$
$D_1 = -\delta_8 - \delta_5 - \delta_6$
$D_2 = \delta_5\delta_8 - \delta_6\delta_7$

where:

$$\delta_1 = -\beta_1, \qquad \delta_2 = 1 + \beta_1,$$

$$\delta_3 = \frac{-2\beta_1^3 + 6\alpha_1\beta_1^2 - 3\alpha_1^2\beta_1}{6},$$

$$\delta_4 = \frac{2\beta_1^3 - 6\alpha_1\beta_1^2 - 6\alpha_1\beta_1 + 3\alpha_2^2\beta_1 + 6\alpha_2\beta_1 + 3\alpha_2^2 + 6\alpha_2 + 2}{6},$$

$$\delta_5 = \frac{\alpha_1^2}{2} - \alpha_1\beta_1, \qquad \delta_6 = \alpha_1\beta_1 + \alpha_1, \qquad \delta_7 = -\frac{\alpha_1^2 + \beta_1^2}{2} + \alpha_1\beta_1$$

$$\delta_8 = \frac{\beta_1^2 + \alpha_2^2}{2} - \alpha_1\beta_1 + \alpha_2 - \alpha_1$$

A.1.3. Three-layer model

$N_1 = 1.223\text{e} - 01$
$N_2 = 2.247\text{e} - 03$
$N_3 = 3.757\text{e} - 06$
$D_1 = 4.557\text{e} - 01$
$D_2 = 2.088\text{e} - 02$

$D_3 = 1.393e-04$

A.1.4. Four-layer model

$N_1 = 1.341e-01$
$N_2 = 3.632e-03$
$N_3 = 2.195e-05$
$N_4 = 1.180e-08$
$D_1 = 4.674e-01$
$D_2 = 2.620e-02$
$D_3 = 3.510e-04$
$D_4 = 7.801e-07$

A.2. DA formulation

A.2.1. One-layer model

$N_1 = 0$
$D_1 = 1/3$

A.2.2. Two-layer model

$N_1 = -1/3(\beta_1 + \beta_1^2)$
$N_2 = 0$
$D_1 = 1/3(1 - \beta_1 - \beta_1^2)$
$D_2 = 1/36(4\beta_1^2 + 5\beta_1^3 + \beta_1^4)$

A.2.3. Three-layer model

$N_1 = 9.842e-02$
$N_2 = 1.030e-03$
$N_3 = 0$
$D_1 = 4.318e-01$
$D_2 = 1.391e-02$
$D_3 = 5.525e-05$

A.2.4. Four-layer model

$N_1 = 1.104e-01$
$N_2 = 1.803e-03$
$N_3 = 5.256e-06$
$N_4 = 0$
$D_1 = 4.437e-01$
$D_2 = 1.776e-02$
$D_3 = 1.326e-04$
$D_4 = 1.772e-07$

References

Agnon, Y., Madsen, P.A., Schaffer, H., 1999. A new approach to high order Boussinesq models. J. Fluid Mech. 399, 319–333.

Gobbi, M.F., Kirby, J.T., 1999. Wave evolution over submerged sills: tests of a high-order Boussinesq model. Coast. Eng. 37, 57–96.

Gobbi, M.F., Kirby, J.T., Wei, G., 2000. A fully nonlinear Boussinesq model for surface waves: Part II. Extension to $O(kh)^4$). J. Fluid Mech. 405, 182–210.

Hsiao, S.-C., Liu, P.L.-F., 2002. Nonlinear water waves propagating over a permeable bed. R. Soc. Lond., A 485 (2022), 1291–1322.

Kanayama, S., Tanaka, H., Shuto, N., 1998. A multi-level model for nonlinear dispersive water waves. In: Edge, B.L. (Ed.), Coast. Eng., vol. 1. ASCE, Reston, VA, pp. 576–588.

Kirby, J.T., Wei, G., Chen, Q., Kennedy, A.B., Dalrymple, R.A., 1998. FUNWAVE 1.0: Fully Nonlinear Boussinesq Wave Model Documentation and User's Manual. Center for Applied Coastal Research University of Delaware, Newark, DE.

Liu, P.L.-F., 1994. Model equations for wave propagation from deep to shallow water. In: Liu, P.L.-F. (Ed.), Advances in Coastal Engineering, vol. 1. World Scientific, Singapore, pp. 125–157.

Lynett, P., Liu, P.L.-F., 2004. A two-layer approach to wave modeling. R. Soc. Lond. A, in press.

Madsen, P.A., Schäffer, H.A., 1998. Higher order Boussinesq-type equations for surface gravity waves—derivation and analysis. R. Soc. Lond., A 356, 1–60.

Madsen, P.A., Sorensen, O.R., 1992. A new form of the Boussinesq equations with improved linear dispersion characteristics: Part II. A slowly varying bathymetry. Coast. Eng. 18, 183–204.

Madsen, P.A., Bingham, H.B., Liu, H., 2002. A new Boussinesq method for fully nonlinear waves from shallow to deep water. J. Fluid Mech. 462, 1–30.

Madsen, P.A., Bingham, H.B., Schäffer, H.A., 2003. Boussinesq-type formulations for fully nonlinear and extremely dispersive water waves: derivation and analysis. R. Soc. Lond., A 459, 1075–1104.

Nwogu, O., 1993. Alternative form of Boussinesq equations for nearshore wave propagation. J. Waterw. Port Coast. Ocean Eng. 119 (6), 618–638.

Schäffer, H.A., Madsen, P.A., 1995. Further enhancements of Boussinesq-type equations. Coast. Eng. 26, 1–14.

Wei, G., Kirby, J.T., Grilli, S.T., Subramanya, R., 1995. A fully nonlinear Boussinesq model for surface waves: Part I. Highly nonlinear unsteady waves. J. Fluid Mech. 294, 71–92.